Article citation info:
Kuczyk M., Jędrzejewski P., Załuski P. Stress analysis of suspended rail vehicle bogie. *Rail Vehicles/Pojazdy Szynowe*. 2022, 1-2, 20-29. https://doi.org/10.53502/RAIL-149199

Rail Vehicles/Pojazdy Szynowe

www.railvehicles.eu

Stress analysis of suspended rail vehicle bogie

Mateusz **Kuczyk** [a, *], Piotr **Jędrzejewski** [a], Paweł **Załuski** [a]

[a] *Faculty of Mechanical Engineering and Ship Technology, Gdansk University of Technology, Poland*

ARTICLE INFO

Received: 9 January 2022
Revised: 3 April 2022
Accepted: 13 April 2022
Available online: 17 April 2022

KEYWORDS

bogie frame
wheelset
stress analysis
monorail
fine element method (FEM)

The main topic of this article is the strength analysis of selected bogie components – the wheelset axle and the frame. Axle calculations were based on the analytical method and were conducted with different types of materials. The finite element method was used for verification of bogie frame construction and loads applied on the frame were calculated according to the PN-EN 13749 norm. The bogie is a part of suspended electric multiple unit which was main matter of authors' master thesis: „The concept of suspended railway engine wagon", conducted on Mechanical Engineering Faculty of Gdansk University of Technology.

1. Vehicle description

Suspended railway is an unusual means of transport used in urban areas. Characteristic feature of such vehicles is that car body hangs several meters above the ground level, so it's completely independent from traffic system. Currently, there can be highlighted two distinctive suspended monorail systems in the world that function as an urban means of transportation: SAFEGE system that originated in France but is used in Japan (the vehicle uses bogies with rubber wheels which move in a closed guidebeam) and Eugen Langen system from German city of Wuppertal (the vehicle is asymmetrically suspended under bogies equipped with a pair of double-flanged wheels cooperating with a single rail). In general, the suspended monorail can be treated as a cheaper alternative to underground railways with a slightly smaller capacity [12, 14].

Considering the above, it seems that vehicles of this type have a greater potential than their marginal use in public transportation. That is why the authors decided to propose their own solution – bidirectional, three-section electric multiple unit (Fig. 1).

Proposed vehicle is suspended symmetrically under the guideway beam which accommodates two steel rails, so the rolling stock uses wheel-rail guidance system (Fig. 2).

Fig. 1. View of proposed suspended railway vehicle [6]

In such a case rail surface is protected from weather conditions that ensures relatively high and stable value of adhesion coefficient. A current collector device is used to supply the rolling stock in electrical power from a third rail. However electrical circuit must be closed and that function is done by wheel-rail contact (a detailed description of proposed solution

* Corresponding author: mateusz.kuczyk@gmail.com (M. Kuczyk)

can be found in other authors' publications [7–9]). Authors' vehicle, in comparison with existing solutions, is characterised by high: capacity, velocity and dynamics. Chosen properties of the rolling stock are presented in Table 1 [6].

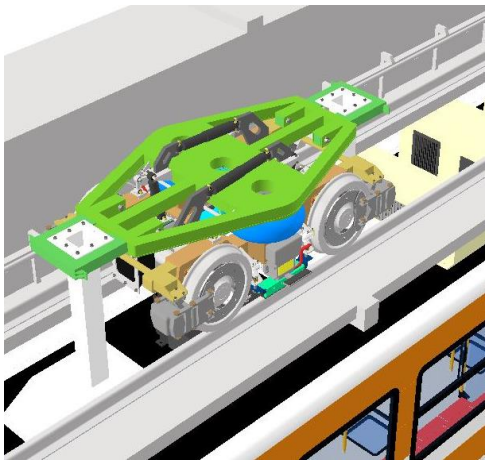

Fig. 2. Rail vehicle bogie in guideway beam [6]

Table 1. Technical specification of suspended EMU

Feature	Unit	Value	Feature	Unit	Value
Overall length	mm	32 580	Maximal acceleration	m/s^2	1.30
Width of the car body	mm	2 500	Maximum braking deceleration	m/s^2	3.60
Height of the car body	mm	3 025	Axle arrangement	–	1A'+1A'+ 1A'
Empty carriage mass	kg	43 611	Wheel diameter	mm	700/750
Maximum vehicle mass	kg	71 811	Bogie centre distance	mm	10 680
Total capacity	–	376	Wheelbase	mm	1 600
Seating capacity	–	80	Track gauge	mm	1 435
Total vehicle power	kW	840	Total mass of the bogie	kg	5 475
Maximum speed	km/h	70	Pressure of the wheelset on a track	t	11,97

For the authors the most important and interesting part of the rolling stock is the bogie (Fig. 3), which could be characterized by:

- low weight, which was achieved by the use of inboard bearings and short wheelbase;
- good running characteristics in a curved track, thanks to: a short wheelbase, elastic wheelset guidance in the bogie frame (quasi-radial adjustment of wheelset in curved track) and wheel flange lubrication system;
- low unsprung mass, which results from the fully sprung gear unit and traction motor, moreover an axle length reduction (inboard bearing);
- high passenger comfort, through two staged suspension system (especially air springs in the secondary suspension);
- good dynamic properties in consequence of using high power motor which also helps the vehicle to move on a steep gradient track.

The rolling stock car body is suspended under three identic two-axle, motor bogies with only one powered axle. Such unusual axle arrangement of the rolling stock is a consequence of using simultaneously double-stage gear and high power motor in bogie with inboard bearings and short wheelbase. Moreover, the lack of space in the bogie frame results in low and longitudinal arrangement of the motor, so its shaft axis lies on the plane passing through both railheads. As key components in terms of safety, bogie frame and wheelset axle was chosen by the authors for the strength analysis. The following chapters present method of load and stress calculation with a short description of the results. At this point it should be noted that the literature devoted directly to suspended monorail vehicles is sparse and largely focuses on issues related to vehicle dynamics (e.g. [3] or [5]) and safety (e.g. [1]).

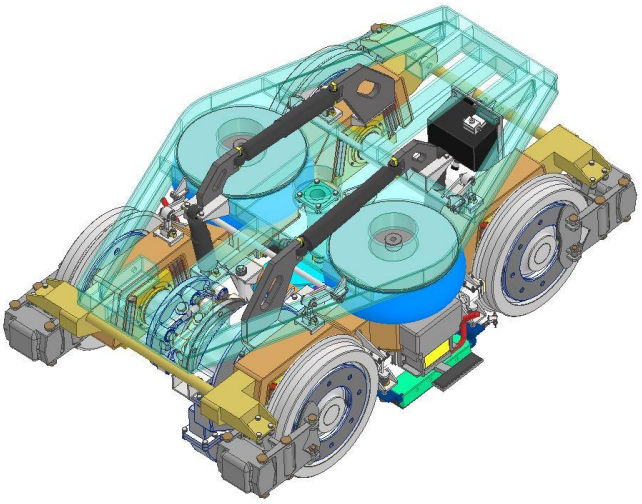

Fig. 3. Bogie construction [6]

2. Axle strength analysis

Inboard bearings, beside mentioned advantages, allow a reduction in bending moment acting on the axle that permitted diameter reduction. However, axleboxes must be fitted onto the axle before the wheels, so access to them is limited. To reduce maintenance activities on the bearings, in the axlebox was used a compact tapered bearing unit with integrated seals and sensors. Only on the wheelset axle strength analysis was conducted and it was based on the analytical method. Wheelset load was defined by calculation methodology according to [11] and [15]. The unusual

construction of the presented vehicle (the centre of gravity significantly below the upper surface of the rail head and the location of the bearings – support points, between the wheels) forced the authors to adapt the formulas to the obtained computational model Fig. 4 – by transforming the moment equation taking into account the opposite turns of moments generated by individual forces.

2.1. Determination of wheelset load

In the calculation was considered stress in five cross-sections (Fig. 4):

- I and V – wheel-mounted area of the axle, diameter 0.12 m;
- II and IV – axlebox-mounted area of the axle, diameter 0.13 m;
- III – centre of the axle, diameter 0.15 m.

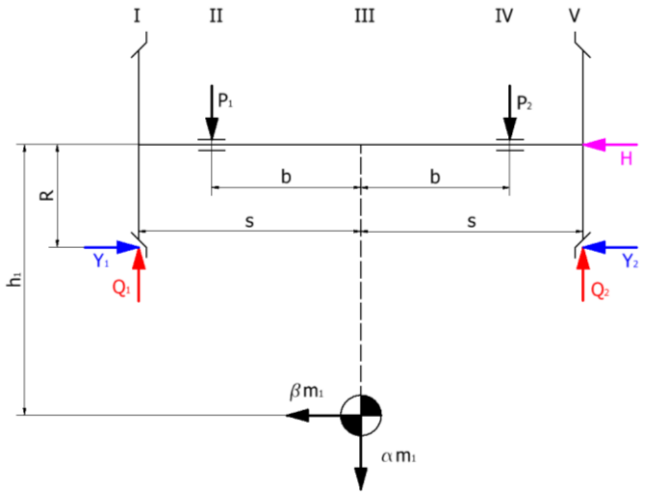

Fig. 4. Calculation model of wheelset [6]

Furthermore, the calculation considered only the worst-case scenario where vehicle is fully loaded. Necessary for load determination were following values (determined on basis of the 3D CAD model of the vehicle prepared by the authors, presented in [6–9]):

- mass of the vehicle per wheelset axle – m_1 = 11,969 kg (in static case and with assumption that vehicle weight is equally distributed between axles);
- distance between axlebox centre plane and the centre of gravity – b = 0.497 m;
- distance between wheelset axle and the centre of gravity – h_1 = 2.750 m;
- wheel rolling radius – R = 0.375 m;
- distance between wheel centre plane and the centre of gravity – s = 0.748 m;
- vertical acceleration – $\alpha = 2.423$ m/s^2;
- horizontal acceleration – $\beta = 1.472$ m/s^2.

The forces from the Fig. 5 were defined and calculated in the following manner:

- P_1 – vertical force acting on the axlebox, represents empty vehicle:

$$P_1 = \frac{\beta \cdot m_1 \cdot h_1 - m_1 \cdot b \cdot (g+\alpha)}{2 \cdot b} = 24\,608 \text{ N} \quad (1)$$

- P_2 – vertical force acting on the axlebox, represents fully loaded vehicle:

$$P_2 = \frac{\beta \cdot m_1 \cdot h_1 + m_1 \cdot b \cdot (g+\alpha)}{2 \cdot b} = 122\,155 \text{ N} \quad (2)$$

- Y_1 – transverse guiding force acting between wheel flange and rail on the side of less loaded axlebox, during motion along a curved track:

$$Y_1 = 0.15 \cdot m_1 \cdot g = 17\,612 \text{ N} \quad (3)$$

- Y_2 – transverse guiding force acting between wheel flange and rail on the side of more loaded axlebox, during motion along a curved track:

$$Y_2 = 0.30 \cdot m_1 \cdot g = 35\,223 \text{ N} \quad (4)$$

- H – horizontal force balancing transverse guiding forces:

$$H = Y_2 - Y_1 = 17\,612 \text{ N} \quad (5)$$

- Q_1 – reaction force acting on the less loaded axlebox:

$$Q_1 = \frac{P_1 \cdot (s+b) + P_2 \cdot (s-b) + R \cdot (Y_1 - Y_2)}{2 \cdot s} = 45\,403 \text{ N} \quad (6)$$

- Q_2 – reaction force acting on the more loaded axlebox:

$$Q_2 = \frac{P_2 \cdot (s+b) + P_1 \cdot (s-b) + R \cdot (Y_2 - Y_1)}{2 \cdot s} = 101\,360 \text{ N} \quad (7)$$

The addition of a vertical reaction forces and forces acting on the axleboxes is equal, so obtained results are correct.

2.2. Determination of axle load

The calculation model (Fig. 5) considers all forces acting on the wheelset, but it assumes that transverse guiding forces are represented by bending moments. Moreover, whole length of the axle was loaded by a torque, which value was equal to tractive torque (it's higher than braking torque even when the highest value of adhesion coefficient has been assumed).The calculations considered three different types of materials of the axle: EA1N, EA4T and 30NiCrMoV12.

The first one is normalized carbon steel and it's the most commonly used material. The second one is quenched and tempered low alloyed steel and it's used for more loaded axles. The last one is high strength alloyed steel which is used in hollow axles of a high-speed railway rolling stocks. High properties of such material permit reducing axle diameter, so unsprung mass of a vehicle is lower. The most important properties, for the strength analysis, of mentioned materi-

als are presented in Table 2 (this and the following tables are at the end of the article), based on [11].

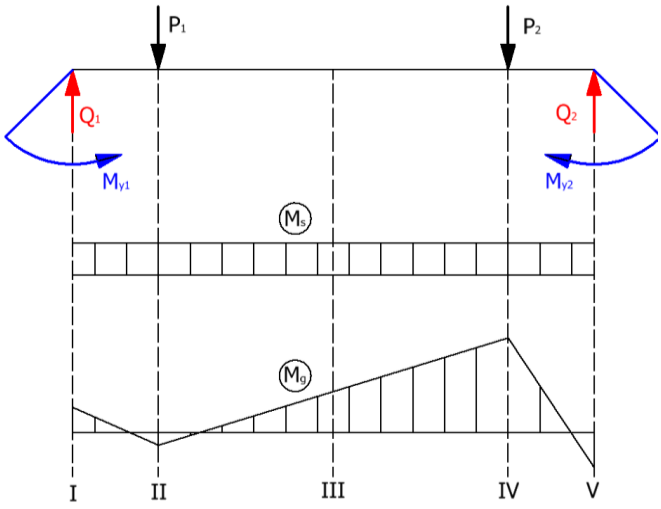

Fig. 5. Calculation model of the wheelset axle [6]

Values of an allowable stress and safety factors was determined by fatigue tests. Additionally, there were considered hollow axles (bore diameter 60 mm) which lower the weight of the wheelset, so it is also a decrease of unsprung mass of a whole bogie. Obtained results were presented in Table 3 [6] and on their basis there could be made only one conclusion – that, with such specified dimensions, it must be solid axle made of EA4T steel or hollow axle made of 30NiCrMoV12. Application of second, more expensive material, allows only for relatively low mass reduction, that it is more reasonable to use a solid axle made of EA4T steel. Additionally in the context of the presented results, it should be noted that the placement of the bearing nodes on the inside of the wheels (troublesome in the context of the operation and maintenance of the vehicle) reduces the value of the maximum torque acting on the axle, and thus also reduces the stresses occurring in it.

3. Frame strength analysis

The bogie frame (Fig. 6) is an internal, closed three-section, welded construction which consists of:

- two closed box-shaped construction side-sills (Fig. 6, No 1) made of 10 mm thick plate of the S355 steel (yield point – 355 MPa, tensile strength – 520 MPa);
- two central cross-bar pipes (Fig. 6, No 2) which are characterized by an outside diameter of 100 mm and inside diameter of 70 mm;
- two pipe headstocks (Fig. 6, No 3) which are characterized by an outside diameter of 60 mm and inside diameter of 30 mm;

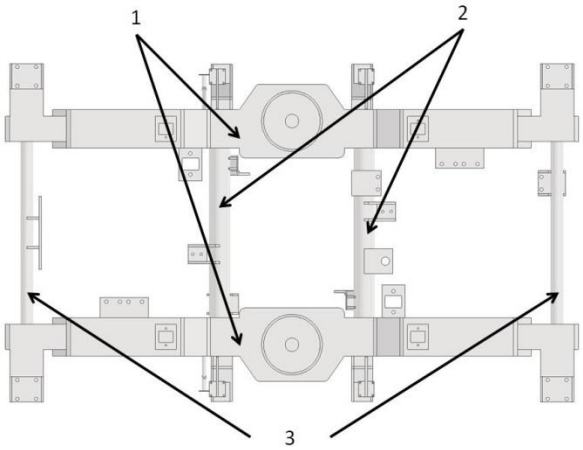

Fig. 6. Bogie frame [6]

The frame weighs only 604 kg. Shape of the side-sills permits chevron springs to wheelset guidance.

Bogie frame strength analysis was based on the standard PN-EN 13749 [10], so there were done static calculations with exceptional and service loads. Additionally, in the calculations were considered cases with frame attachments loads.

3.1. Static analysis

In order to determine the loads acting on the frame following values were used (on the basis of the 3D CAD model of the vehicle prepared by the authors, presented in [6–9]):

- total mass of empty vehicle – M_v = 43 611 kg;
- mass of maximal load – m_p = 28 200 kg;
- mass of real service load – m_{pe} = 21 075 kg;
- mass of the bogie – m^+ = 4 800 kg;
- number of axles in the bogie – n_a = 2;
- number of bogies in the rolling stock – n_b = 3;
- roll coefficient – α = 0.1;
- bounce coefficient – β = 0.2.

In carried out calculations on the bogie frame acted:

- vertical forces caused by suspended mass acceleration, with:
  - exceptional load:

$$F_{z1max} = \frac{1.4 \cdot g \cdot (M_v + m_p - n_b \cdot m^+)}{n_a \cdot n_b} \quad (8)$$

  - service load:

$$F_{z1} = \frac{g \cdot (M_v + 1.2 \cdot m_{pe} - n_b \cdot m^+)}{n_a \cdot n_b} \quad (9)$$

  - transverse forces resulting from:
  - exceptional load:

$$F_{ymax} = 2 \cdot \left(10^4 + \frac{(M_v + m_p) \cdot g}{3 \cdot n_a \cdot n_b}\right) \quad (10)$$

  - service load:

$$F_y = 2 \cdot \left(\frac{(M_v + 1.2 \cdot m_{pe}) \cdot g}{3 \cdot n_a \cdot n_b}\right) \quad (11)$$

- longitudinal forces resulting from:
  - exceptional load:

$$F_{xmax} = 0.1 \cdot (2 \cdot F_{z1max} + m^{+} \cdot g) \quad (12)$$

  - service load:

$$F_{x} = 0.05 \cdot (2 \cdot F_{z1} + n_{b} \cdot m^{+} \cdot g) \quad (13)$$

  - forces resulting from a track twist.

Previous formulas were based on calculation methodology presented in the [2] and [16]. Considering that the above calculations relate to the case of a static frame load, the location of the center of gravity of the vehicle below the rail head (with the use of a special suspension of the car body – forces resulting from the weight of the vehicle are applied to the upper surfaces of the side-sills), does not affect the calculation method, which directly allows on the adaptation of formulas from the cited sources. All load cases, with number values of applied forces, were compared in the Table 4 [6]. Different values of the vertical forces in service cases are caused by α and β coefficients, so value of:

- 62 376 N refer to $F_{z1/2} \cdot (1 - \alpha - \beta)$;
- 80 198 N refer to $F_{z1/2} \cdot (1 + \alpha - \beta)$;
- 98 020 N refer to $F_{z1/2} \cdot (1 - \alpha + \beta)$;
- 115 842 N refer to: $F_{z1/2} \cdot (1 + \alpha + \beta)$.

In the calculation model (Fig. 7) were imposed boundary conditions, so all planes supported on the chevron springs in primary suspension were fixed. In cases which considered a track twist, half of the supported planes were left free and they were loaded with rail reaction forces.

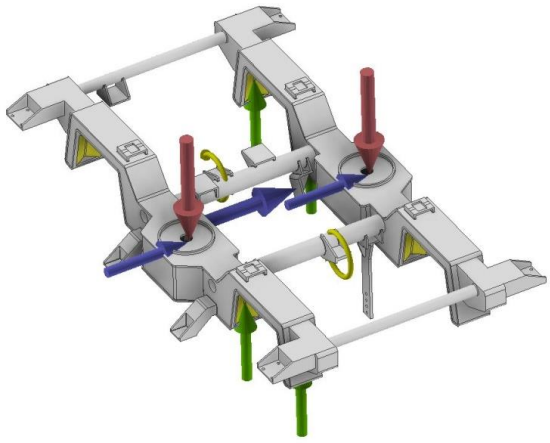

Fig. 7. Load of the bogie frame in exceptional and service cases [6]

Vertical and a part of the transverse forces were applied on the interfaces between bogie frame and secondary suspension. Rest of the transverse load was applied on the car body movements limiter. Longitudinal load was applied on the place of traction rods fastened (Fig. 8).

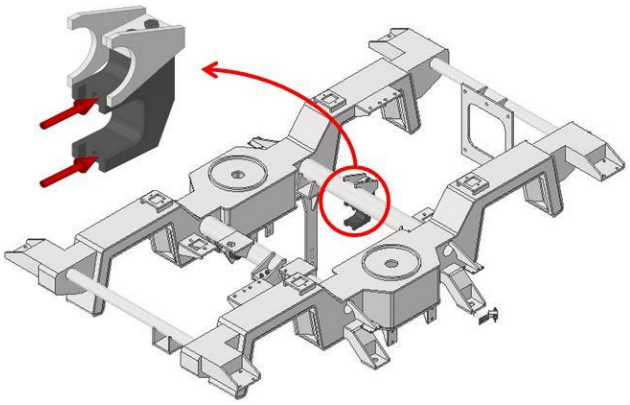

Fig. 8. Assembly of traction rod in the bogie frame [6]

Those rods are attached to the frame central crossbars by additionally screwed parts, so in strength analysis of the frame every longitudinal force was replaced by equivalent bending moment. Bogie frame model mesh consists of tetrahedral solid elements in parabolic order and it's characterized by: number of fine elements 452 077 and number of nodes 872 906. This settings was not changed for all considered load cases also for two additional cases with frame attachments loads. In addition, the calculations did not take into account the strength of the welds in the welded joints in the frame, assuming therefore, that if properly made, these areas will not have worse strength parameters than the original material. Table 6 [6] consists of chosen results of the static analysis. On their base we could observe that stress values slightly exceed safety limit of 200 MPa only in individual calculation nodes (as already mentioned, the yield point of used steel is 355 MPa, which translates into a minimum safety factor of 1.8), and the area of their concentration is the central part of the side-sills. Also bogie frame displacements values are fully acceptable. The biggest displacement was concentrated around attachment points of the secondary suspension, where forces were attached. The exception from this principle were cases, which additionally considered loads resulting from twisted track, where the greatest values of the displacement where concentrated at the ends of side-sills (in which fixed boundary were replaced by rail reaction forces). In the same time stress is concentrated around primary suspension seats, therefore there is need to change calculation model or side-sills construction.

3.2. Attachments loads

Two additional cases in the bogie frame static analysis were considered with forces and moments, which resulted from attachment units work. Case M1 refers to breaking fully loaded vehicle with maximal deceleration by disc brake and track brake systems.

Case M2 refers to hypothetical situation of a speed increase with maximum acceleration in a curved track.

The calculations considered loads (Fig. 9) coming from:

- magnetic track brake – vertical force generated by electromagnet Q_{DHS} and bending moment resulting from friction force between drag shoe and rail M_{HHS1};
- disc brake – bending moment M_{dbu} resulting from multiplication between friction force F_T and distance from that force to reference point R_H;
- gear unit and motor – in case M1 it's gravity force and in case M2 it's gravity force enlarged by dynamic reactions, which result from drive system work;
- anti-roll bar.

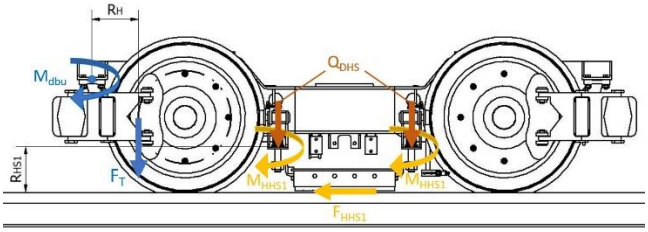

Fig. 9. Frame load from the operation of the braking system [6]

The last load was calculated as follows [4]:

$$F_{anti} = \frac{k_s \cdot \arcsin\frac{L_{anti}\cdot\sin\alpha}{2L}}{L_{anti}\sqrt{1-\left(\frac{L_{anti}\cdot\sin\alpha}{2L}\right)^2}} \text{ [N]} \qquad (14)$$

where: k_s – torsional rigidity of the anti-roll bar [Nm/rad], L_{anti} – length of the torsion bar [m], L – length of the torsion arm [m], α – permissible tilt angle of the car body [°].

The calculation model with applied additional loads is presented in the Fig. 10 (Table 4 and 5 [6]). Obtained results, in a graphic form, are listed in Table 7 [6]. In case M1 stresses are concentrated on a brakes equipment attachments points, especially in the elements of track brake mount that results from relatively large distance between them and frame sidesills. Case M2 shows asymmetrical load of the bogie frame which is a result of only one powered wheelset in the bogie.

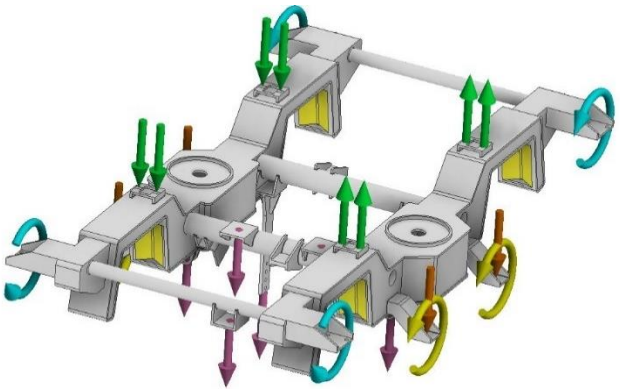

Fig. 10. Loads on the bogie frame attachments [6]

4. Recapitulation

In this article authors focused on the bogie frame and wheelset axle strength analysis, so in the same time description of the whole vehicle was strictly limited, and it can be find in another authors' publications: [7–9]. Aforementioned bogie elements were chosen, because they are crucial for vehicle safety. Generally, obtained stress and displacement values are acceptable, which confirms appropriate construction of inspected parts. Moreover, use of internal frame resulted in bending moments reduction. It is important to state that the authors restrained strength analysis only to static cases. In the further development of the bogie construction dynamic loads and fatigue strength should be taken into account which probably would impose some changes in original structure. Fatigue calculations are especially important when we consider that bogies which use chevron springs in wheelsets guidance, sometimes has problems with fatigue cracking of bogie frame in the area of aforementioned springs. Good example of such situation is 37 AN bogie [13]. In such cases there is a necessity to use additional element which would fasten bogie frame parts from both sides of axlebox. Moreover, the authors didn't exclude the possibility of using one bogie between each section of the vehicle (in such case it would be suspended under four bogies), that would reduce the force value distributed on both elements.

Table 2. Characteristics of steels for wheelset axle

Feature	EA1N	EA4T	30NiCrMoV12
Yield strength [MPa]	320	420	834
Tensile strength [MPa]	550	650	932
Allowable stress on the solid axle body surface [MPa]	200	240	300
Allowable stress on the bore surface of hollow axle [MPa]	80	96	120
Allowable stress on the fitted areas of solid axle [MPa]	120	144	b/d
Allowable stress on the fitted areas of hollow axle [MPa]	110	132	175
Allowable stress on the bearings mounting places of hollow axle [MPa]	94	113	120
Permissible safety factor [–]	1.20	1.33	1.22

Table 3. Results of the strength calculations of the railway axle

No.	Feature	EA1N	EA4T	EA4T (d)	30Ni...(d)
–	Permissible safety factor [–]	1.20	1.33	1.33	1.22
I	Torsional stress [MPa]	38.81	38.81	41.40	41.40
	Bending stress [MPa]	38.93	38.93	41.53	41.53
	Equivalent stress [MPa]	77.68	77.68	82.86	82.86
	Allowable stress [MPa]	120.00	144.00	132.00	175.00
	Actual safety factor [–]	1.54	1.85	1.59	2.11
II	Torsional stress [MPa]	30.53	30.53	31.98	31.98
	Bending stress [MPa]	11.93	11.93	12.50	12.50
	Equivalent stress [MPa]	54.20	54.20	56.78	56.78
	Allowable stress [MPa]	120.00	144.00	113.00	120.00
	Actual safety factor [–]	2.21	2.66	1.99	2.11
III	Torsional stress [MPa]	19.87	19.87	20.39	20.39
	Bending stress [MPa]	25.69	25.69	26.37	26.37
	Equivalent stress [MPa]	42.95	42.95	44.08	44.08
	Allowable stress [MPa]	200.00	240.00	96.00	120.00
	Actual safety factor [–]	4.66	5.59	2.18	2.72
IV	Torsional stress [MPa]	30.53	30.53	31.98	31.98
	Bending stress [MPa]	67.00	67.00	70.18	70.18
	Equivalent stress [MPa]	85.35	85.35	89.40	89.40
	Allowable stress [MPa]	120.00	144.00	113.00	120.00
	Actual safety factor [–]	1.41	1.69	1.26	1.34
V	Torsional stress [MPa]	38.81	38.81	41.40	41.40
	Bending stress [MPa]	77.86	77.86	83.05	83.05
	Equivalent stress [MPa]	102.86	102.86	109.72	109.72
	Allowable stress [MPa]	120.00	144.00	132.00	175.00
	Actual safety factor [–]	1.17	1.40	1.20	1.59

Table 4. Load cases in static analysis

	Case	F_{z1} [N]	F_{z2} [N]	F_y [N]	F_x [N]	T_w [N]
Exceptional loads	N1	131 414	131 414	98 274		
	N2	131 414	131 414	98 274		55 005
	N3	131 414	131 414		30 992	55 005
	N4	131 414	131 414	98 274	30 992	
Service loads	E1	89 109	89 109	75 102		
	E2	89 109	89 109	75 102		55 005
	E3	89 109	89 109		15 974	55 005
	E4	89 109	89 109	75 102	15 974	
	E5	115 842	62 376	75 102		
	E6	115 842	62 376	–75 102		
	E7	80 198	98 020		15 974	
	E8	115 842	80 198			
	E9	62 376	98 020	–75 102		55 005
	E10	80 198	115 842		15 974	55 005
Attachments loads	M1	131 414	131 414			
	M2	89 109	89 109	75 102	15 974	

Table 5. Attachments load cases

	Case	M_{dbu} [Nm]	F_{HS} [N]	M_{HHS1} [Nm]	F_{anti} [N]	F_{p+s} [N]
Attachments loads	M1	5 696	36 000	1 452	97 397	11 978
	M2				97 397	310 000

Table 6. Results of the strength analysis of the bogie frame

	Von Misses stresses [MPa]	Displacement [mm]
N1	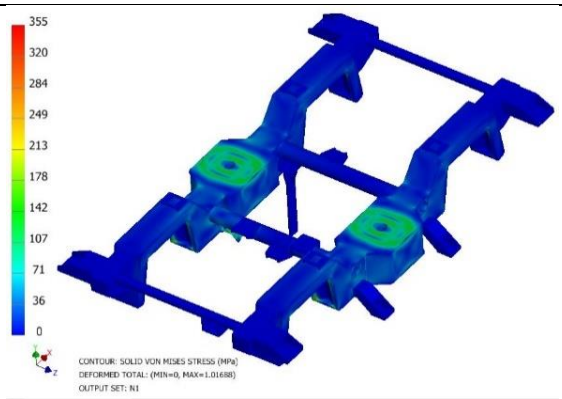	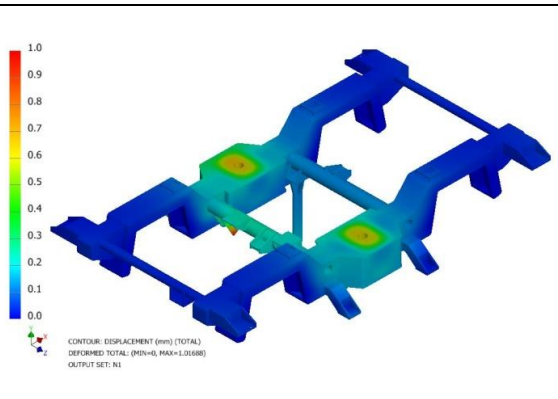
N2	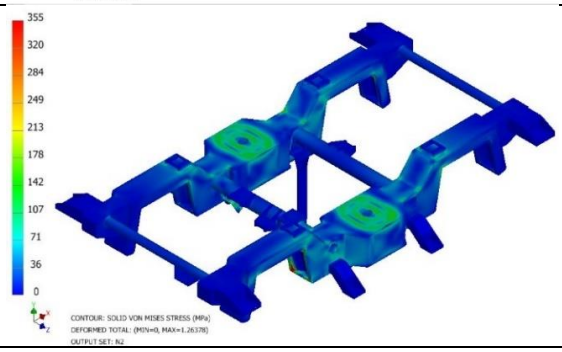	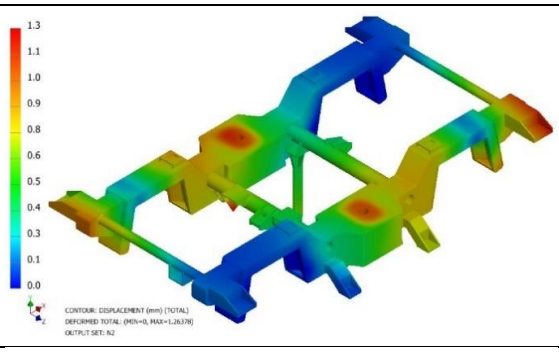
N3	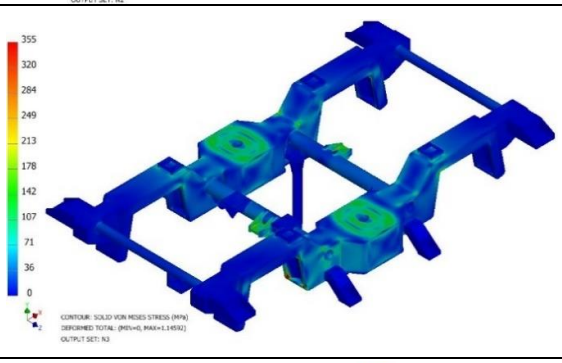	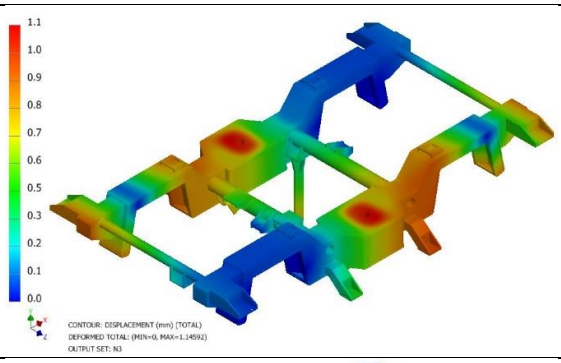
N4	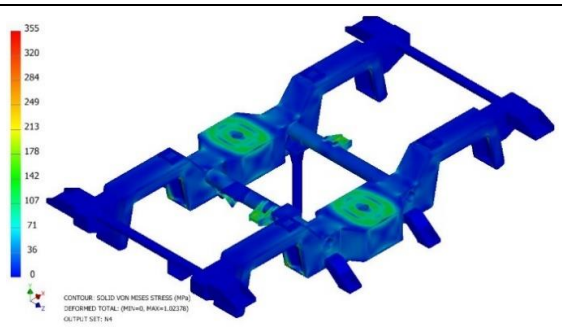	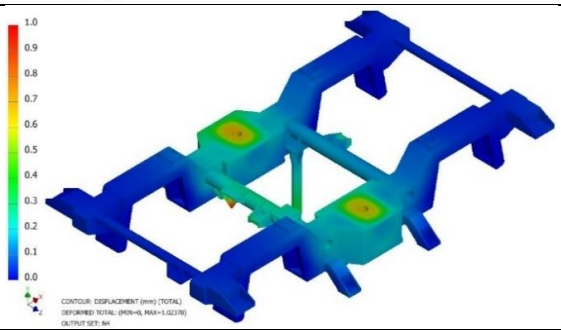
E5	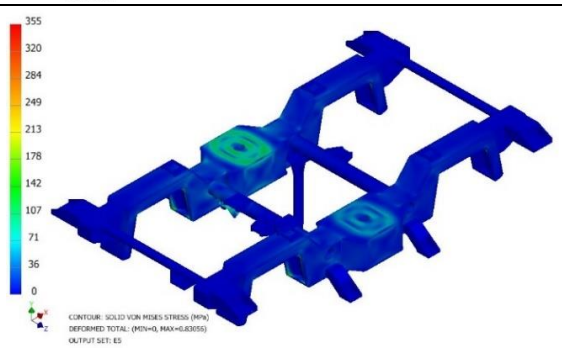	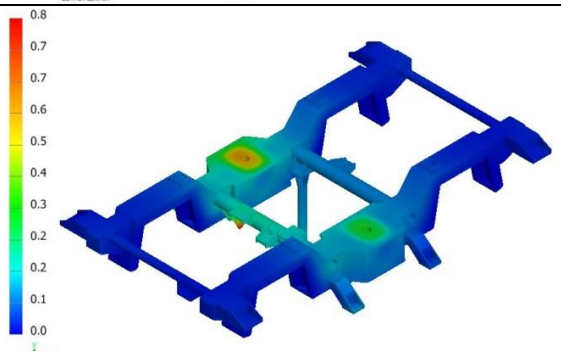

Table 7. Results of the strength analysis – cases M1 and M2

	Von Misses stresses [MPa]	Displacement [mm]
M1	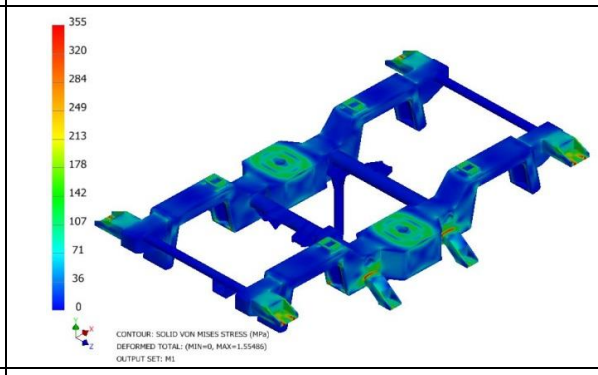	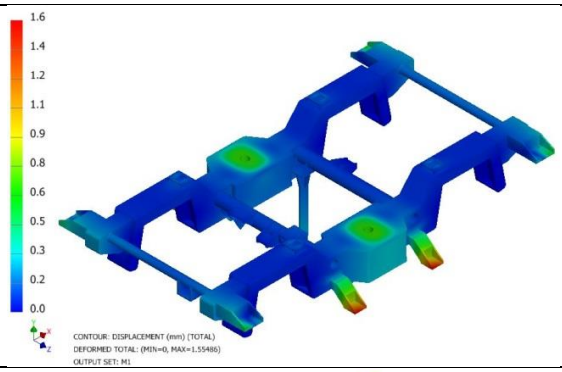
M2	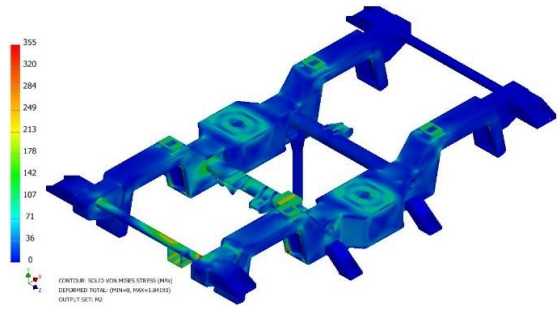	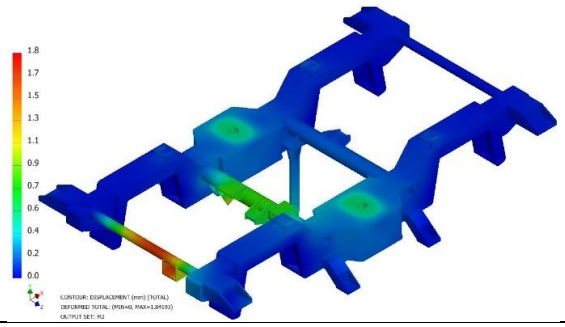

Nomenclature

b	distance between axlebox centre plane and the centre of gravity
F_{p+s}	load caused by work of population system
F_{anti}	force resulting from anti-roll bar
F_x	longitudinal forces resulting from service load
F_{xmax}	longitudinal forces resulting from exceptional load
F_y	transverse forces resulting from service load
F_{ymax}	transverse forces resulting from exceptional load
F_{z1}	vertical forces caused by suspended mass acceleration, with service load
F_{z1max}	vertical forces caused by suspended mass acceleration, with exceptional load
g	gravitational acceleration
H	horizontal force balancing transverse guiding forces
h_1	distance between wheelset axle and the centre of gravity
k_s	torsional rigidity of the anti-roll bar
L	length of the torsion arm
L_{anti}	length of the torsion bar
M_{dbu}	bending moment caused by work of disc brake
M_{HHS1}	moment resulting from friction force between drag shoe of magnetic track brake and rail
M_v	total mass of empty vehicle
m_p	mass of maximal load
m_{pe}	mass of real service load
m_1	mass of the vehicle per wheelset axle
m^+	mass of the bogie
n_a	number of axles in the bogie
n_b	number of bogies in the rolling stock
P_1	vertical force acting on the axlebox, represents empty vehicle
P_2	vertical force acting on the axlebox, represents fully loaded vehicle
Q_1	reaction force acting on the less loaded axlebox
Q_2	reaction force acting on the more loaded axlebox
R	wheel rolling radius
s	distance between wheel centre plane and the centre of gravity
T_w	force resulting from track twist
Y_1	transverse guiding force acting between wheel flange and rail on the side of less loaded axlebox, during motion along a curved track
Y_2	transverse guiding force acting between wheel flange and rail on the side of more loaded axlebox, during motion along a curved track

Bibliography

[1] Bao Y., Li Y., Ding J. A case study of dynamic response analysis and safety assessment for a suspended monorail system. *International Journal of Environmental Research and Public Health*. 2016, 13, 1121. https://doi.org/10.3390/ijerph13111121

[2] Bharadwaj C. Stress analysis of bogie frame structure. *Master thesis*. *Blekinge Institute of Technology*, Karlskrona 2017. https://www.diva-portal.org/smash/get/diva2:1194122/FULLTEXT03.pdf (accessed on 20.09.2020).

[3] Cai C., He Q., Zhu S. et al. Dynamic interaction of suspension-type monorail vehicle and bridge: numerical simulation and experiment. *Mechanical Systems and Signal Processing*. 2019, 118, 388-407. https://doi.org/10.1016/j.ymssp.2018.08.062

[4] Chen D., Sun S., Li Q. Strength evaluation of a bogie frame by different methods. *Mechanical Engineering Science*. 2019, 1(1), 54-64. https://doi.org/10.33142/me.v1i1.662.

[5] Guo Q., Wang P., Chen J. et al. Dynamic analysis on suspended monorail vehicle passing through turnouts. *IOP Conference Series: Materials Science and Engineering*. 2018, 439, 042078. https://doi.org/10.1088/1757-899X/439/4/042078

[6] Jędrzejewski P., Kuczyk M. Koncepcja wagonu silnikowego kolei podwieszanej. *Master thesis*. Gdańsk 2020.

[7] Kuczyk M., Jędrzejewski P., Załuski P. Evaluation of suspended rail vehicle movement parameters. *Rail Vehicles/Pojazdy Szynowe*. 2021, 3, 20-29. https://doi.org/10.53502/RAIL-143045

[8] Kuczyk M., Jędrzejewski P., Załuski P. The construction of suspended rail vehicle bogie. *Rail Vehicles/Pojazdy Szynowe*. 2021, 4, 1-13. https://doi.org/10.53502/RAIL-144534

[9] Kuczyk M., Jędrzejewski P., Załuski P. The concept of suspended urban rail vehicle. *Rail Vehicles/Pojazdy Szynowe*. 2021, 2, 52-66. https://doi.org/10.53502/RAIL-139982

[10] Mancini G., Cera A. Design of railway bogies in compliance with new EN 13749 European standard. http://www.railway-research.org/IMG/pdf/609.pdf (accessed on 18.09.2020)

[11] Mancni G., Corbizi A., Lombardo F. et al.. Design of railway axle In compliance with the European Norms: high strength alloyed steel compared to standard steel. http://www.railway-research.org/IMG/pdf/617.pdf (accessed on 25.08.2020)

[12] SAFEGE monorail: https://kamakura-enoshima-monorail.jp/fun/index.html (accessed on 05.04.2022)

[13] Safety alerts from 19.02.2016 and 10.06.2016. https://www.utk.gov.pl/pl/monitorowanie/alerty-bezpieczenstwa/alerty-bezpieczenstwa-o-1/6988,Alerty-bezpieczenstwa-opublikowane-w-2016-roku.html (accessed on: 20.10.2020)

[14] Schwebebahn: https://schwebebahn.de/en/ (accessed on 05.04.2022)

[15] Sobaś M. Analytical determination of load capacity of the freight wagon wheelset axle with axle journal dimensions ϕ120×179 mm. *Rail Vehicles/Pojazdy Szynowe*. 2019, 3, 48-59. https://doi.org/10.53502/RAIL-138539

[16] Sobaś M. Badania wytrzymałościowe wózka 11 ANC. *Rail Vehicles/Pojazdy Szynowe*. 2010, 2, 31-41. https://doi.org/10.53502/RAIL-139720